28. W. W. Cochran, M. Wikelski, in *Birds of Two Worlds*, P. Marra, R. Greenberg, Eds. (Johns Hopkins Press, Baltimore, 2004), in press.
29. R. Sandberg, *et al.*, *Auk* **119**, 201 (2002).
30. S. T. Emlen, *Anim. Behav.* **18**, 215 (1970).
31. W. Wiltschko, R. Wiltschko, *Z. Tierpsychol.* **39**, 265 (1975).
32. W. Wiltschko, R. Wiltschko, *J. Comp. Physiol.* **177**, 363 (1995).
33. T. Ritz, S. Adem, K. Schulten, *Biophys. J.* **78**, 707 (2000).
34. T. Alerstam, *J. Exp. Biol.* **130**, 63 (1987).
35. K. J. Lohmann, S. D. Cain, S. A. Dodge, C. M. F. Lohmann, *Science* **294**, 364 (2001).
36. K. P. Able, *Nature* **299**, 550 (1982).
37. J. B. Phillips, F. R. Moore, *Behav. Ecol. Sociobiol.* **31**, 189 (1992).
38. K. P. Able, M. A. Able, *J. Comp. Physiol.* **177**, 351 (1995).
39. R. C. Beason, *Ethology* **91**, 75 (1992).
40. W. Wiltschko, R. Wiltschko, *Z. Tierpsychol.* **37**, 337 (1975).
41. V. P. Bingman, W. Wiltschko, *Ethology* **77**, 1 (1988).
42. E. Batschelet, *Circular Statistics in Biology* (Academic Press, London, 1981).
43. We are indebted to A. Raim for lifelong help; E. Gwinner for inspiration; and G. Swenson, G. Swenson, and J. Bruggemann for help with light measurements and thank M. Bowlin, N. Sapir, A. Medina, W. Cochran, J. Cochran, J. Mandel, and S. David for their help, support, and understanding during this intensive project and W. Wiltschko for constructive comments on the manuscript. Supported by the National Geographic Society (M.W.), Princeton University (M.W.), Volkswagen Stiftung (H.M.), Oldenburg University (to H.M.) and NSF (GB 3155 and 6680 to W.W.C.).

Supporting Online Material
www.sciencemag.org/cgi/content/full/304/5669/405/DC1
Materials and Methods
Figs. S1 and S2
Tables S1 and S2

20 January 2004; accepted 10 March 2004

Southern Ocean Iron Enrichment Experiment: Carbon Cycling in High- and Low-Si Waters

Kenneth H. Coale,[1]* Kenneth S. Johnson,[2] Francisco P. Chavez,[2] Ken O. Buesseler,[3] Richard T. Barber,[4] Mark A. Brzezinski,[5] William P. Cochlan,[6] Frank J. Millero,[7] Paul G. Falkowski,[8] James E. Bauer,[9] Rik H. Wanninkhof,[10] Raphael M. Kudela,[11] Mark A. Altabet,[12] Burke E. Hales,[13] Taro Takahashi,[14] Michael R. Landry,[15] Robert R. Bidigare,[16] Xiujun Wang,[1] Zanna Chase,[2] Pete G. Strutton,[2] Gernot E. Friederich,[2] Maxim Y. Gorbunov,[8] Veronica P. Lance,[4] Anna K. Hilting,[4] Michael R. Hiscock,[4] Mark Demarest,[5] William T. Hiscock,[7] Kevin F. Sullivan,[10] Sara J. Tanner,[1] R. Mike Gordon,[1] Craig N. Hunter,[1] Virginia A. Elrod,[2] Steve E. Fitzwater,[2] Janice L. Jones,[5] Sasha Tozzi,[8,9] Michal Koblizek,[8] Alice E. Roberts,[6] Julian Herndon,[6] Jodi Brewster,[1] Nicolas Ladizinsky,[1,6] Geoffrey Smith,[1] David Cooper,[1] David Timothy,[12] Susan L. Brown,[16] Karen E. Selph,[16] Cecelia C. Sheridan,[16] Benjamin S. Twining,[17] Zackary I. Johnson[18]

The availability of iron is known to exert a controlling influence on biological productivity in surface waters over large areas of the ocean and may have been an important factor in the variation of the concentration of atmospheric carbon dioxide over glacial cycles. The effect of iron in the Southern Ocean is particularly important because of its large area and abundant nitrate, yet iron-enhanced growth of phytoplankton may be differentially expressed between waters with high silicic acid in the south and low silicic acid in the north, where diatom growth may be limited by both silicic acid and iron. Two mesoscale experiments, designed to investigate the effects of iron enrichment in regions with high and low concentrations of silicic acid, were performed in the Southern Ocean. These experiments demonstrate iron's pivotal role in controlling carbon uptake and regulating atmospheric partial pressure of carbon dioxide.

The Southern Ocean exerts a major control on the partial pressure of carbon dioxide (pCO_2) in the atmosphere. Because rates of photosynthesis and biological carbon export are low in Antarctic waters, macronutrients are largely unused, and upwelled CO_2 entering the atmosphere (*1*, *2*) sustains the relatively high interglacial atmospheric pCO_2 of the present day (*3*).

Southern Ocean surface waters contain extremely low iron concentrations (*4*, *5*), and the low rates of primary production have been attributed to iron deficiency. Recent open-ocean iron enrichment experiments demonstrate the validity of this hypothesis in the Southern Ocean (*6*, *7*). Martin (*8*) proposed that natural variations in the atmospheric iron flux ultimately regulate primary production in the Southern Ocean and influence the pCO_2 of the atmosphere, thereby potentially affecting the radiative balance of the planet. Syntheses of models, field observations, and paleoceanographic data (*3*, *9*, *10*, *11*, *12*) support a role for iron-regulated changes in Southern Ocean macronutrient use. Indeed there is a strong inverse correlation between iron-rich dust, marine production, and atmospheric pCO_2 over the past four glacial cycles as recorded in Antarctic ice cores (*13*). These observations support the "iron hypothesis" as proposed by Martin (*8*), yet the magnitude of the iron enrichment effect on marine production and atmospheric pCO_2 remains uncertain.

Although all Southern Ocean surface waters have high concentrations of nitrate and phosphate, silicic acid concentrations differ markedly from north to south. Subantarctic waters north of the Antarctic Polar Front Zone (APFZ) have low Si concentrations (1 to 5 μM), whereas high Si (>60 μM) is found to the south (fig. S1). Diatoms, which require Si for growth, are believed responsible for much of the carbon export from the surface to the deep sea (*14*). In

[1]Moss Landing Marine Laboratories, 8272 Moss Landing Road, Moss Landing, CA 95039–9647, USA. [2]Monterey Bay Aquarium Research Institute, 7700 Sandholdt Road, Moss Landing, CA 95039, USA. [3]Department of Marine Chemistry and Geochemistry, Woods Hole Oceanographic Institution, Woods Hole, MA 02543, USA. [4]Nicholas School of the Environment and Earth Sciences, Duke University, 135 Duke Marine Lab Road, Beaufort, NC 28516, USA. [5]Marine Science Institute and the Department of Ecology, Evolution, and Marine Biology, University of California, Santa Barbara, CA 93106, USA. [6]Romberg Tiburon Center for Environmental Studies, San Francisco State University, 3152 Paradise Drive, Tiburon, CA 94920–1205, USA. [7]Rosenstiel School of Marine and Atmospheric Research, University of Miami, 4600 Rickenbacker Causeway, Miami, FL 33149–1098, USA. [8]Environmental Biophysics and Molecular Ecology Program, Institute of Marine and Coastal Sciences and Department of Geology, Rutgers University, 71 Dudley Road, New Brunswick, NJ 08901–8521, USA. [9]Virginia Institute of Marine Science, Route 1208 Greate Road, Gloucester Point, VA 23062, USA. [10]Atlantic Oceanographic and Meteorological Laboratory/National Oceanic and Atmosphereic Administration, 4301 Rickenbacker Causeway, Miami, FL 33149, USA. [11]University of California at Santa Cruz, 1156 High Street, Santa Cruz, CA 95064, USA. [12]School for Marine Science and Technology, University of Massachusetts, 706 South Rodney French Boulevard, New Bedford, MA 02744–1221, USA. [13]College of Oceanic and Atmospheric Sciences, Oregon State University Corvallis, OR 97331, USA. [14]Lamont-Doherty Earth Observatory, Columbia University, 61 Route 9W, Palisades, NY 10964–1000, USA. [15]Scripps Institution of Oceanography, University of California, San Diego, 9500 Gilman Drive, La Jolla, CA 92093–0227, USA. [16]Department of Oceanography, University of Hawaii at Manoa, 1000 Pope Road, Honolulu, HI 96822, USA. [17]State University of New York, Stony Brook, NY 11794, USA. [18]Massachusetts Institute of Technology, 48-336A MIT, 15 Vassar Street, Cambridge, MA 02139, USA.

*To whom correspondence should be addressed. E-mail: coale@mlml.calstate.edu

previous iron enrichment experiments, diatoms have responded with the greatest increase in biomass (*6*, *7*, *15*, *16*). The large silicic acid gradient across the APFZ (*17*) suggests that iron enrichment would cause diatoms to bloom to the south of the APF, whereas nonsiliceous phytoplankton species would likely dominate in waters to the north. The majority (~65%) of the Southern Ocean surface waters lie in the northern subantarctic region with low silicic acid but high nitrate. If increased macronutrient use does play a role in controlling climate, then large increases in nitrate-based photosynthesis and carbon export should occur after iron enrichment in both the high and low silicic acid waters of the Southern Ocean.

Two previous open-ocean iron enrichment experiments have been conducted in the Southern Ocean, one in the Australian sector [Southern Ocean iron release experiment (SOIREE) (*6*)] and the other in the Atlantic sector [Eisen (iron) experiment (EisenEx) (*7*)] (Fig. 1). Both experiments demonstrated that Southern Ocean phytoplankton respond directly to iron addition by increasing primary production and biomass, with a corresponding reduction in pCO_2 and nitrate concentrations. However, both experiments were performed in waters of moderate silicic acid concentrations (~5 to ~25 μM) just south of the APFZ. Considerable Si depletion occurs each year during natural phytoplankton blooms in this zone (*18*, *19*). The prior experiments do not clarify the potential for Fe and Si interactions to regulate the carbon cycle in the very low–Si waters to the north of the APFZ or in the high-Si waters to the south, where little or no Si depletion occurs (*18*). This experiment, the Southern Ocean Iron Experiment (SOFeX), was designed to address that uncertainty.

Experimental conditions. We enriched two distinct regions. The north patch was characterized by high nitrate (~20 μM) and low silicic acid concentrations (<3 μM), whereas the south patch location had high nitrate (~28 μM) and high silicic acid concentrations (~60 μM). The average mixed layer temperatures and depths at the north and south patch sites were 5° to 7°C and 40 m and −0.5°C and 45 m, respectively. Three ships were used to perform the experiments. Both initial site surveys and iron injections were carried out by research vessel (RV) *Revelle* with the use of methods previously described (*20*). Multiple enrichments were performed on areas of 15 km by 15 km (three additions of iron to ~1.2 nM in the north and four additions of iron to ~0.7 nM in the south) to produce a sustained amount of iron in the experimental areas (*21*) that exceed saturation for phytoplankton growth (*22*). Similar to other Southern Ocean iron enrichments (*6*, *7*), iron persisted in the patch at high concentrations, relative to surrounding waters, throughout the experiment (*23*). The iron-enriched patches were subsequently sampled in the north and south by RV *Revelle* and RV *Melville* and in the south by U.S. Coast Guard Research Ice Breaker *Polar Star*. The details of the northern and southern patch enrichments are shown in tables S1 and S2, respectively, and the ship tracks with regional nutrient fields are shown in fig. S1, A and B, with local hydrography and ship tracks shown in fig. S1C.

Patch dilution and mixing. The north patch was deployed in a region with many fronts and evolved from a square into a narrow filament 7 km wide by at least 340 km long by day 38 (Fig. 2A). In contrast, the south patch slowly expanded in all directions throughout the observational period to an area of ~2380 km² after 20 days (Fig. 2B). Such mixing will act to dilute products of bloom development [chlorophyll a (Chl a), particulate organic carbon (POC), etc.] yet enrich the reactants for bloom formation (Si, NO_3^-, etc.). Two methods were used to calculate the resultant dilution of the iron-enriched waters with the unenriched waters surrounding each patch: (i) The physical

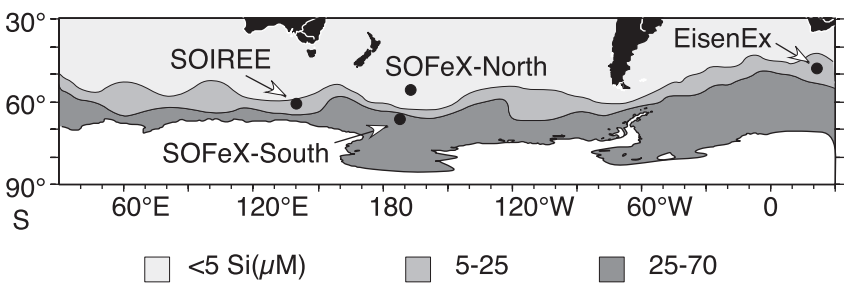

Fig. 1. The Southern Ocean showing the waters with low (<5 μM), intermediate (5 to 25 μM), and high (25 to 70 μM) silicic acid concentrations together with the locations of the recent Southern Ocean enrichment experiments (SOIREE, EisenEx, and SOFeX).

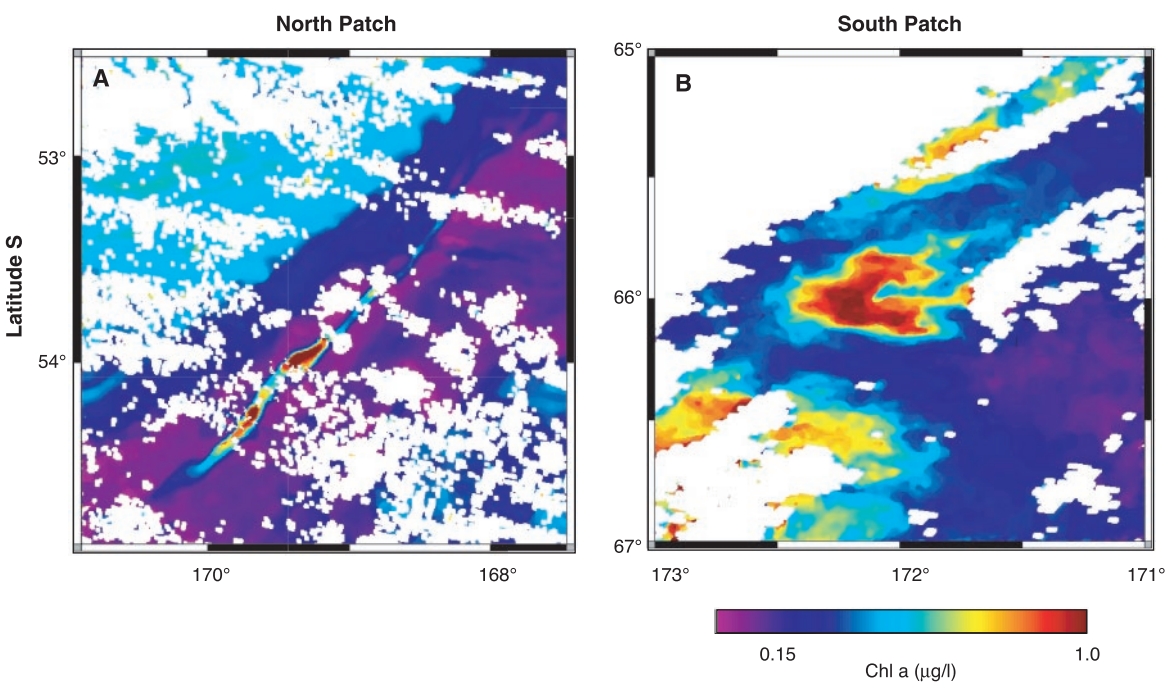

Fig. 2. (**A**) MODIS (Moderate Resolution Imaging Spectroradiometer) image of the north patch on day 28 of the experiment, showing an extremely elongated and narrow band of chlorophyll extending over 250 km. (**B**) SeaWIFS (Sea-Viewing Wide Field-of-View Sensor) image of the south patch on day 20 of the south patch experiment.

strain was calculated from satellite images of patch deformation (*24*). (ii) The loss of SF_6, injected as a conservative tracer and corrected for outgassing, was used to calculate dilution. Both methods yielded similar results. The rate of dilution of the north patch was 0.11 day^{-1} (strain) and 0.10 day^{-1} (SF_6). Dilution estimates for the south patch were 0.086 day^{-1} (strain) and 0.03 day^{-1} to 0.07 day^{-1} (SF_6). SF_6-derived mixing rates varied because of inhomogeneities within the patch and analytical variability. Dilution rates of 0.11 and 0.08 were used for north and south patches, respectively. These rates are substantially lower than those observed during the equatorial iron enrichment experiments (IronEx I and II), where patch dilution was as high as 0.4 day^{-1} because of shear from large horizontal velocity gradients, yet similar to those observed during SOIREE (0.07 day^{-1}) (*24*).

Dilution of the patch with unenriched waters will reduce the magnitude of geochemical signals that are produced inside the patch as a result of iron-stimulated phytoplankton growth. For a dilution rate of 0.1 day^{-1}, the initial concentration of an inert tracer is reduced by some 20-fold over the course of 30 days, corresponding to a mixing loss of 0.1 day^{-1}. However, dilution has a much smaller impact on a geochemical signal such as the accumulation of POC, which is produced by an exponentially increasing phytoplankton population (fig. S2). Most of that geochemical signal will be produced near the end of the 30-day period, because the phytoplankton population will be largest at that time. As a result, a simple numerical simulation of the SOFeX patches, based on the observed rates of growth and mixing, indicates that a 0.1 day^{-1} dilution rate reduced geochemical signals by two to four times. Further, dilution will act on all geochemical signals in about the same manner. Ratios that are determined from the temporal change in chemical concentrations remain unchanged. However, dilution of a patch may have a much larger impact on physiological processes that are operating in a near-limiting condition. Horizontal dilution of the northern patch appeared to be a major source of silicic acid that sustained diatom growth (see below). This effect is analogous to silicic acid supply from vertical mixing and upwelling, the dominant supply over much larger areas. Except in Table 1, we report all geochemical changes without correction for dilution.

After each addition of iron, its concentration decreased (Fig. 3, A and B) at a rate that was nearly equal to that of SF_6. The SF_6 concentration decreased because of dilution and because of gas exchange with the atmosphere (~0.07 day^{-1}). Given the similarity of the total loss rates for each chemical, dissolved iron must also have had additional sinks other than dilution, which are presumably biological uptake and scavenging. These processes must have occurred at a rate of ~0.05 day^{-1}.

The biological response. Before iron release, photosynthetic competency [F_v/F_m (*25*)] was low in both north and south patches (0.20 and 0.25, respectively), indicating severe nutrient limitation of phytoplankton photosynthesis. After iron enrichment, F_v/F_m increased to 0.5 in the north patch and to 0.65 in the south patch, indicating that the photosynthetic community was relieved from iron limitation (*26*) (fig. S3). Maximum rates of photosynthesis (P_{opt}) also increased with iron addition, from 0.29 to 6.9 mmol C m^{-3} day^{-1} in the north patch and from 0.29 to 4.6 mmol C m^{-3} day^{-1} in the south patch (Fig. 4). The increase in photosynthetic competency was slower to develop (2 to 3 days) than in IronEx I and II (2 to 3 hours) (*27*), but similar to the response measured during the SOIREE experiment (2 to 3 days) (*28*) and consistent with temperature being the main factor driving this difference (*29*). Both iron enrichment and temperature effects were apparent in phytoplankton community growth rates (*30*), which increased from ambient amounts of ~0.2 day^{-1} to >0.3 day^{-1} in the south patch and from 0.3 day^{-1} to >0.5 day^{-1} by day 12 in the north patch. During SOIREE, phytoplankton growth rates increased similarly from 0.08 day^{-1} to 0.20 day^{-1} (*31*), and the relative magnitude of the increase was comparable to those observed in IronEx II (*32*).

Although phytoplankton biomass outside the patches remained roughly constant throughout the observational period, Chl a concentration in the euphotic zone increased by factors of 10 to 20 inside north and south patches, respectively (Fig. 3, C and D, and fig. S4). Both patches were easily observed from space by ocean color satellite sensors when clouds permitted (Fig. 2, A, day 28 north patch, and B, day 20 south patch). Such conditions only prevailed for 1 day during the south experiment, whereas a composite image of the northern patch could be constructed from multiple satellite passes. The response of the community

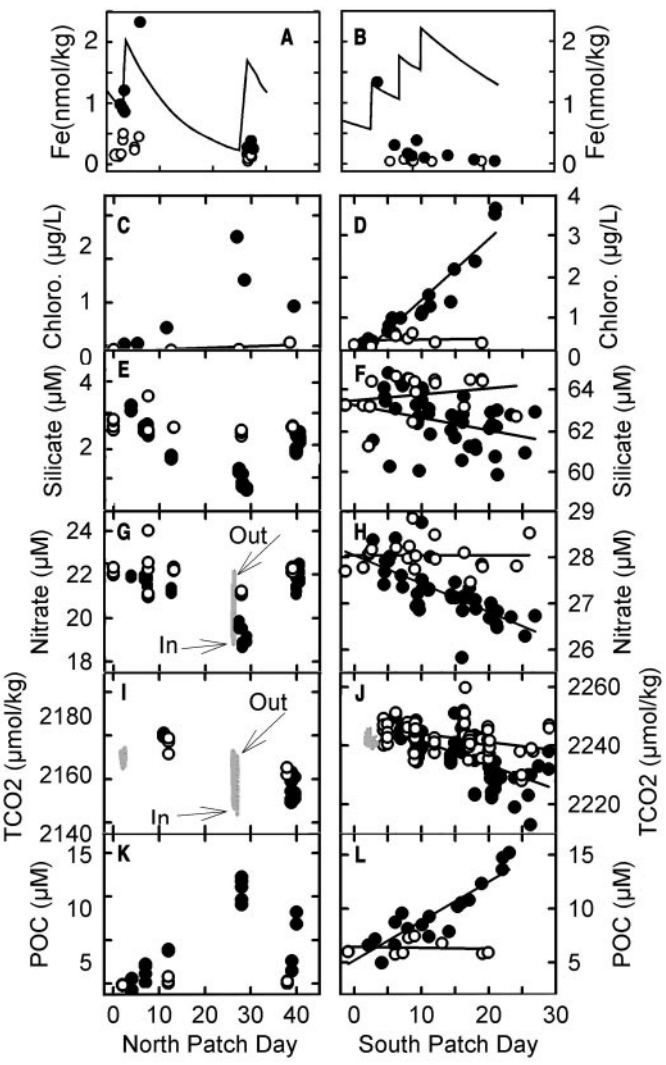

Fig. 3. (**A** to **L**) Evolution of major geochemical signals (iron, chlorophyll, Si, nitrate, $NTCO_2$, and POC) in north (left) and south (right) patch experimental sites as a function of day of experiment. The lines in (A) and (B) refer to the expected dissolved iron concentrations based on dilution as determined by SF_6. Multiple additions explain the sawtooth behavior of these curves. Whereas good agreement between expected and measured iron exists immediately after most injections, the difference between expected and observed reflects particle formation and biological uptake. The details of the injections can be found in tables S1 and S2. Gray dots in (G) are continuous nitrate measurements made with pumping SeaSoar in transects across the patch. Gray dots in (I) and (J) are normalized (to salinity 35), and TCO_2 values were determined from continuous pCO_2 measurements and observed alkalinity values in the north and south patches, respectively. It should be noted that RV *Melville* reoccupation of the north patch (last data points) encountered only slightly elevated values of SF_6 and thus these latter points do not reflect maximum "inside" stations. These latter values do not, therefore, reflect a decrease in biological activity. Open circles, outside patch; solid circles, inside patch.

structure in the northern patch was toward larger cells (>5 μm), whereas the size structure of the phytoplankton community remained unchanged in the south. In the north patch, enhanced growth was evident for flagellated phytoplankton groups (prymnesiophytes, pelagophytes, and dinoflagellates) as well as the diatom *Pseudonitzschia* spp. By day 38, diatom biomass showed the largest change relative to initial values but represented somewhat less than half of the total (fig. S5).

The south patch was dominated (at both inside and outside stations) by diatoms, and Chl a increased by a factor of 20. Despite high silicic acid concentrations in the south patch (Fig. 3F), the diatoms in both patches were thin-walled, poorly silicified, and therefore, lightly ballasted (*14*). Moreover, on the basis of single-cell, x-ray fluorescence analysis (*33*), the silicic acid cell quotas of diatoms in the south patch decreased about 50% after the initial iron addition and remained lower than silicic acid quotas in diatoms outside of the patch. Whether this corresponds to an adjustment of frustule thickness by individual species or a shift to species with inherently thinner frustules is presently unknown. A shift to lower silicic acid quotas may keep diatoms in surface waters with high iron (*34*). In contrast, iron-limited diatoms can generally increase silicification, perhaps to facilitate access to higher iron concentrations in deeper water (*34*, *35*).

Phytoplankton growth using nitrate requires greater cellular iron requirements as compared to growth on more reduced forms of nitrogen (*36*). Alleviation of iron deficiency after fertilization resulted in enhanced rates of nitrate uptake at both sites. Absolute rates of nitrate uptake increased by a factor of ~15 in the north patch and ~25 in the south patch relative to outside control regions. Addition of Fe also increased biomass-specific NO_3^- uptake rates by factors of 5 and 10 in the north and south patches, respectively (Fig. 5, A and B), a result similar to those reported for iron-amended bottle experiments conducted previously in the Southern Ocean (*37*, *38*).

There were clear decreases (~2 μM) in the nitrate concentration of the mixed layers in both the north and south patches (Fig. 3, G to H). The proportion of nitrate to total nitrogen (NO_3^-, NO_2^-, NH_4^+, and urea) uptake was measured during day-long ^{15}N incubations as a proxy for new production. This value (*f* ratio) increased from a range of 0.1 to 0.2 to a ratio of 0.5 to 0.6 in the southern patch and 0.3 to 0.4 in the northern patch, clearly indicating that sufficient iron allows for the greater use of nitrate reserves (Fig. 5, A and B).

Absolute rates of silicic acid uptake increased by a factor of 11 in the north patch and by a factor of 4 in the south patch. Specific uptake rates increased by factors of 5.6 and 6.6 in the north and south patches, respectively. The maximum specific rates observed near the end of each experiment imply maximum doubling times for diatoms in the north patch (2 days) that were twice as long as those for the south patch (1 day), despite the significantly warmer surface waters in the north, possibly because of Si limitation in the low-Si waters of the subantarctic.

The addition of iron caused a steep decrease in silicic acid:nitrate uptake ratios in the diatom-dominated south patch, from an average of 8.1 ± 1.5 outside the patch to 2.1 ± 0.5 inside the patch, consistent with observations that release from iron stress shifts silicic acid–to–

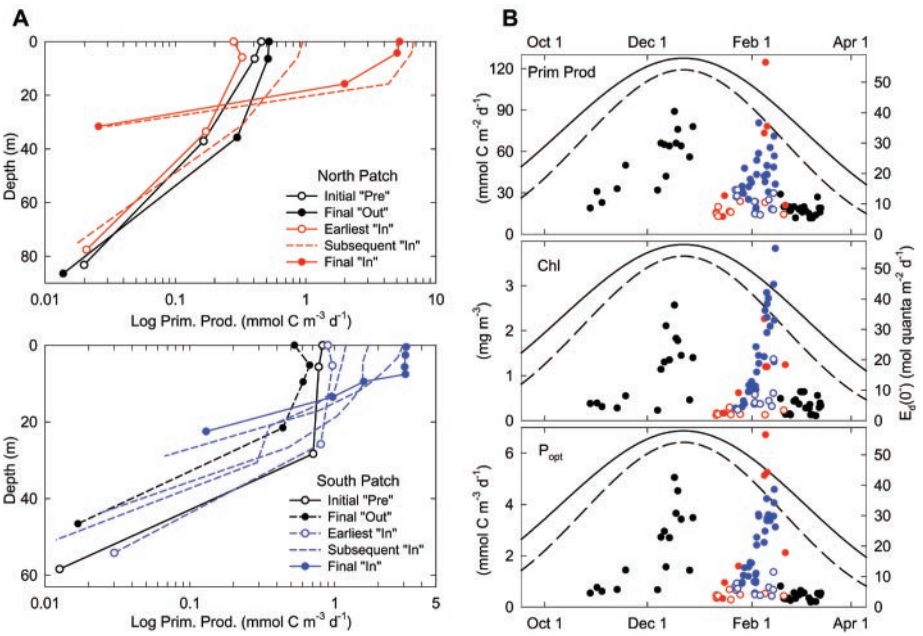

Fig. 4. Primary production in the north and south patches. (**A**) Depth profiles indicating differences between inside and outside stations. For north patch black symbols, initial pre and final out stations were sampled on patch days –1.7 and 27, respectively; for north patch red symbols, earliest in, subsequent in (s), and final in were sampled on patch days 2, 3, 27, and 29, respectively. For south patch black symbols, initial pre and final out were sampled on patch days 9 and 32; for south patch blue symbols, earliest in, subsequent in (s), and final in stations were sampled on patch days 14, 17, 19, 27, and 33, respectively d, day. (**B**) All productivity measurements are relative to the values obtained during the JGOFS AESOPS study, indicating iron enrichment enhances primary production beyond values normally seen for any time of year. P_{opt} is the maximal daily photosynthesis occurring within the euphotic zone. Black circles, AESOPS 1997 to 1998; red solid circles, north in; red open circles, north out; blue solid circles, south in; blue open circles, south out. $E_d(0^-)$ is the downwelling irradiance just below the surface of the ocean.

Table 1. Concentration changes observed within the experimental sites relative to values observed outside each patch on day 30. South patch values were calculated from the difference in regression lines fit to inside and outside patch measurements at patch day 30 (Fig. 3). North patch values were calculated from the difference in measurements made inside and outside the patch on patch day 28. DIC:NO_3^- ratios are calculated from the TCO_2/NO_3^- depletion. Correction for gas exchange was not made. The balance terms reflect changes in carbon due to vertical export of POC or accumulation of DOC and were estimated from the model increase of POC and an export ratio of 0.5 (Fig. 5) for north and south patches. Units are in μg l^{-1} for Chl a, μmol kg^{-1} for TCO_2, and μM for all other values except DIC:NO_3^-, for which the units are mol mol^{-1}. Error limits are 90% confidence levels. Values in parentheses represent estimated dilution corrected values as per the model presented in table S2. For the dilution-corrected Chl a values, a net growth rate of 0.18 day^{-1} (versus 0.11 day^{-1} for POC) was used in the north patch, and a net growth rate of 0.16 day^{-1} (versus 0.08 day^{-1} for POC) was used in the south patch. GE indicates gas exchange.

	North patch	South patch
Chlorophyll a	2.6 (18)	4 (17)
TCO_2 depletion	–15 ± 2 (–60)	–16 ± 6 (–42)
Nitrate depletion	–2.0 ± 0.2 (–12)	–1.9 ± 0.7 (–10)
Silicic acid depletion	–1.5 (–12)*	–4.0 (–14)
DIC:NO_3^- molar depletion ratio	7.7 ± 1.2 (9.0 ± 0.1)†	8.9 ± 5
POC accumulation	8.5 ± 0.8 (60)	11 ± 3 (42)
Biogenic silica accumulation	1.2 (12)	4.2 (14)
CO_2 gas exchange	2	2 ± 1
Balance (–TCO_2 – POC + GE)	9 ± 3 (32)	7 ± 7 (21)

*There was not this much initial silicic acid present at the north patch, yet dilution with outside waters provided a continual source. †The DIC:NO_3^- value in parentheses for the north patch was derived from measurements made in the upper 30 m with the pumping SeaSoar on patch day 28 (Fig. 6).

nitrate uptake ratios toward values closer to Redfield proportions (*34*, *39*). In the north patch where the phytoplankton was dominated by nondiatoms, silicic acid:nitrate uptake ratios were nearly identical inside and outside the patch (0.86 ± 0.35 inside versus 1.0 ± 0.38 outside).

Although rates of silicic acid uptake increased by a factor of 4 in the northern patch, the low silicic acid concentrations in the north (Fig. 3E) strongly limited silica production, which likely diminished the diatom response to iron addition. These results have their basis in shipboard experiments in which diatoms received enrichments of silicic acid and their subsequent uptake was measured (*40*) (Fig. 5, C and D). Whereas only one case of an increase in uptake was evident in south patch silicic acid enrichments, the north patch consistently showed 180 to 380% increases in uptake when silicic acid was added, indicating sufficient ambient silicic acid in the southern but not the northern patch.

The demand for silicic acid in the north patch appeared to be met by dilution of the patch with outside waters by the end of the experiment. Silicic acid uptake rates measured directly in north patch waters on patch day 39 were 0.22 μmol Si l^{-1} day^{-1}. A strain rate of 0.11 day^{-1} and a Si concentration difference of 3 μM outside and 0.8 μM inside will add 0.24 μmol l^{-1} day^{-1} to the patch. Thus, biological uptake of Si was nearly balanced by the amount of Si added by mixing. It appears that biogenic silica production in the north patch was regulated by Si added by mixing with surrounding waters. The supply of silicic acid via mixing was thought to have contributed to the longevity (>50 days) of the SOIREE bloom [(*6*), based on satellite data], but in situ data were not available to confirm this. Silicic acid limitation can explain why the depletion of silicic acid and the increase in biogenic silica in the north patch were each less than half those observed in the south patch (Table 1) despite similar initial siliceous biomass in each area and the warmer temperatures in the north.

Despite the low silicic acid concentrations, maximum rates of primary production in the north patch were about double those in the south patch (Fig. 4A). Much of this difference likely stems from the higher temperatures in the north patch and demonstrates that the low silicic acid concentrations do not necessarily limit primary productivity or POC accumulation (Fig. 3, K and L) after iron addition to low silicic acid waters.

The photosynthetic and biomass response to iron additions were compared with observations from the U.S. Joint Global Ocean Flux Study (JGOFS) Antarctic Environment and Southern Ocean Process Study (AESOPS) that sampled largely between the APFZ and the Southern Antarctic Circumpolar Current Front along 170°W, where blooms are more frequent (Fig. 4B). Phytoplankton production rates inside both patches were clearly above the maximum values observed during AESOPS (*18*), and production continued to increase linearly throughout the experiment. This would indicate that conditions in the Southern Ocean rarely exist naturally to promote the maximum production that was observed under iron-replete conditions.

The profiles of primary production in Fig. 4A are consistent with the development of light limitation also observed during EisenEx (*7*). The highest primary production values are seen near the surface. As the bloom developed, subsurface production rates decreased to values lower than ambient. Measurements of in situ irradiance indicate that the diffuse attenuation of solar radiation roughly doubled in each patch over the course of the experiments, with the depth of the 1% light level shoaling from 83 m to 32 m in the north (28 days) and from 58 m to 23 m in the south (33 days). This suggests that light limitation as a result of self-shading may slow production. Furthermore, the ratio of photoprotective to photosynthetic carotenoids in the south patch decreased by a factor of 3 during bloom development, suggesting a transition from iron- toward light-limited growth inside the patch (*41*).

Carbon export and nutrient use ratios. Biological processes driven by photosynthesis may shift CO_2 from the atmosphere into the ocean by four mechanisms: (i) increased air-to-sea CO_2 flux from reduced pCO_2 because of increased photosynthesis, (ii) enhanced carbon export resulting from an increase in the ratio of carbon to nitrogen in exported particles (*3*, *10*), (iii) a shift in the mixed-layer remineralization ratios whereby nitrogen is regenerated more efficiently than carbon, and (iv) a change in the species composition of the export community. Iron influenced all of these mechanisms in our experiments.

Total inorganic carbon concentrations (TCO_2) were clearly depleted in both the north and south patches (Fig. 3, I and J), as iron increased photosynthetic rates and nitrate consumption. The TCO_2 depletion in the south patch, estimated from direct measurements of TCO_2 in bottle samples collected over the course of the experiment, was 16 ± 6 [90% confidence interval (CI)] μmol kg^{-1}. Continuous measurements of pCO_2 from the *Revelle* survey were combined with measurements of titration alkalinity to estimate the change in TCO_2 in the north patch of 15 ± 2 (90% CI) μmol kg^{-1} (Fig. 3I). The corresponding decrease in pCO_2 within both of the fertilized patches was ~40 μatm.

A budgeting approach can be used to estimate export from both patches. After correction for the flux of CO_2 across the air-sea interface, the decrease in TCO_2 exceeds the accumulation of POC (Fig. 3, K and L) after ~30 days by 8 ± 3 μmol kg^{-1} in the north patch and 7 ± 7 μmol kg^{-1} in the south patch (Table 1). The balance of the missing TCO_2 can be accounted for by an increase in the dissolved organic carbon (DOC)

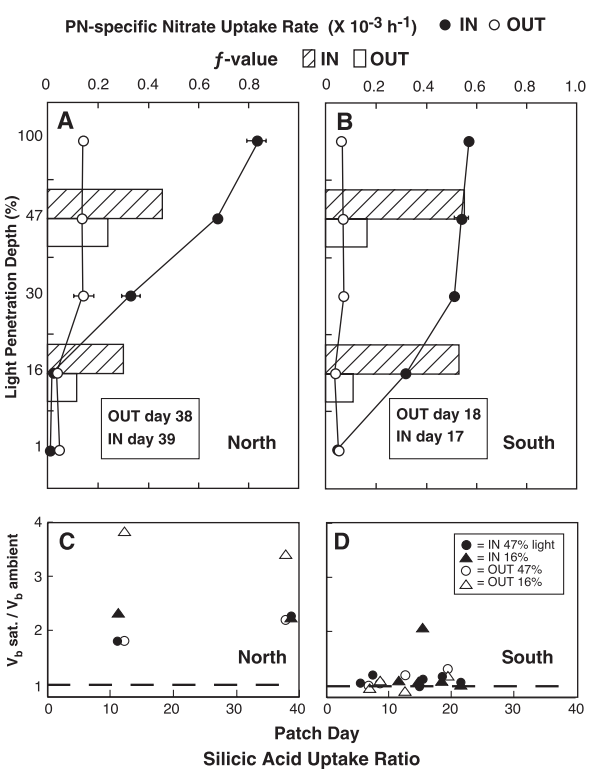

Fig. 5. (**A** and **B**) Depth profiles of biomass (PN)-specific NO_3^- uptake rates (V), determined during 24-hour incubations in Plexiglas (Rohm GmbH and Company Kg. Kirschenalee, Germany) acrylic glass incubators under simulated in situ light and temperature conditions and with the use of ultraclean trace-metal techniques for samples collected within and outside (control waters) of the Fe-enriched patch north (A) and south (B) of the APFZ. The *f* values [$f = V_{NO3}/(V_{NO3} + V_{NH4} + V_{NO2} + V_{Urea})$] were determined at the 47 and 16% light depths with the use of tracer-level isotopic enrichments and are not corrected for the effects of isotopic dilution. Error bars represent the range of duplicate samples ($n = 2$). Hatched bars indicate inside stations; open bars indicate outside stations. North patch inside station was sampled on patch day 39; outside station was sampled on patch day 38. South patch inside stations were sampled on patch day 17; outside station was sampled on patch day 18. (**C** and **D**) Enhancement of the specific rate of biogenic silica production, V_b (*40*), by saturating additions of silicic acid [+21 μM $Si(OH)_4$ in the north patch (C) and +42 μM $Si(OH)_4$ in the south patch (D)]. Values > 1 indicate that ambient silicic acid concentrations were not supporting the maximum potential of the microplankton for silicic acid uptake. Analytical and experimental uncertainties require that the enrichment ratio exceed 1.2 to be significant. Solid fill denotes in stations; open, out patch stations. Circles denote experiments at the 47%, and triangles, 16% light depths. The dashed line indicates a ratio of one.

pool or by vertical export via sinking particles from the patch. Buesseler *et al*. (*42*) measured increased POC export (~10 mmol m^{-2} day^{-1}) from the southern patch at the end of the experiment. This export corresponds to a loss of ~6 μmol C kg^{-1} from a 50-m mixed layer over 30 days and accounts for our observed imbalance between TCO_2 reduction and POC production. Although insufficient POC and DOC measurements for the north patch are available from this experiment to resolve the fate of the missing carbon at this time, aggregates of the diatom *Pseudonitzchia* spp. and colonial *Phaeocystis* spp. were observed by day 38 in the north patch, consistent with the potential for significant carbon export. Furthermore, observations from an autonomous drifter (*43*) indicate that a large flux event resulted from iron enrichment in the north patch. Although northern production and biomass were dominated by nonsilicious phytoplankton, the communities driving export production shifted toward diatoms in the north but remained diatom-dominated in the south.

Measurements in other regions of the Southern Ocean suggest that ecosystems may export carbon in greater-than-Redfield proportions (*44*). The drawdown of TCO_2 in each iron-fertilized patch exceeded values expected from the observed amount of nitrate consumption and a Redfield ratio of 6.6 (Table 1). The best evidence for elevated C:N ratios of exported particles was obtained during a survey of the north patch with a pumping SeaSoar system (*45*) on patch day 28. This survey shows a dissolved inorganic carbon (DIC):NO_3^- drawdown ratio of 9.0 ± 0.12 (95% CI, model II regression of normalized TCO_2 versus NO_3) (Fig. 6A), which is conservative because it was uncorrected for gas exchange. The DIC:NO_3 removal ratio (6.9 ± 0.6) estimated from hydrographic measurements in the Pacific sector of the Southern Ocean is indistinguishable from Redfield (*43*). This is unexpected given that C:N ratios are usually observed to decline in populations recently relieved from iron deficiency (*38*).

In contrast, the ratios of C:N in suspended particles from the north patch and south patch mixed-layer stations were 6 and 5.2, respectively, values near Redfield and consistent with the preferential nitrate uptake by iron-stimulated phytoplankton (Fig. 6B). These ratios are consistent with removal ratios observed elsewhere yet are much lower than those observed in the water column during both experiments. If particulate material is responsible for the majority of the vertical flux of carbon from the mixed layer, then these results strongly suggest that shallow differential remineralization of nitrogen relative to carbon is the likely explanation. Such differential remineralization has been observed for nitrogen relative to silicon during AESOPS experiments in this same area (*46*).

Synthesis. The SOFeX experiments produced several unexpected results: (i) Because of silicic acid limitation, a strong differential response to added iron was observed, with nonsilicious phytoplankton dominating production in the north and diatoms dominating in the south. (ii) In spite of diatom growth limitation, carbon budgets, radioactive proxies for flux (*42*), and free-vehicle observations (*43*) indicate carbon flux from both sites, suggesting a stronger role for iron-limited carbon removal from these waters. (iii) Differential remineralization of nitrogen relative to carbon could result in a carbon flux greater than would be predicted from available nitrate.

Relative to iron fertilizations in equatorial waters (*22*), both north and south patch blooms were slow to develop, and biomass continued to increase throughout the observational period. This rate of biomass increase is consistent with previous iron enrichments in Antarctic waters (*6*, *7*), indicating that temperature as well as patch dilution may act together to slow biomass accumulation. Only 10% of the nitrate available for phytoplankton growth was consumed. In contrast, phytoplankton consumed 20 μM nitrate during an iron enrichment experiment in the subarctic Pacific (*16*). In that experiment, the mixed layer was only 10 m deep, with a temperature of 9.5°C. We speculate that light limitation produced by a combination of a deep mixed layer (>40 m) and self-shading attenuated the development of blooms in the north and south patches. Much shallower mixed layers (~20 m) were observed during the U.S. JGOFS experiments near the south patch site (*20*), yet seasonally and spatially variable mixed layers are characteristic of these waters (*47*). Thus, it is possible that much greater consumption of nitrate can be achieved during periods with lower wind speeds. Loss of iron does not appear to have limited production. Iron concentrations in the north patch were 0.2 nM above ambient concentrations on patch day 28 (*23*), which is consistent with loss predominantly by mixing.

These results stand in contrast to some of the recent JGOFS findings that indicate phytoplankton communities in the Southern Ocean south of the APFZ are not limited by iron availability (*48*). Further, some of us have reported (*18*, *49*) that silicic acid availability within the APFZ may limit diatom biomass, growth, and carbon export. Low silicic acid concentrations do appear to limit diatom growth in the north, but the results indicate that iron limitation plays the dominant role in phytoplankton rate processes in the vast subantarctic region north of the APFZ. Low silicic acid, however, would curtail the contribution of diatoms to new production under prolonged iron enrichment. The <1 μM silicic acid concentrations in the north patch would prevent diatoms from consuming more than 5% of the remaining nitrate, given the silicic acid:nitrate molar depletion ratio of 0.8:1 occurring in the north patch (Table 1).

Although differences in silicic acid concentrations may lead to differences in the export community that develops under iron-replete conditions, iron remains the proximal control on total phytoplankton biomass. Both north and south of the APFZ enhanced growth of the larger phytoplankton taxa followed iron addition. Large blooms led to a decoupling between production and grazing, resulting in a drawdown of the major nutrients and carbon. However, the development of large blooms is intimately linked to the mixed layer depth and light limitation. Although the larger diatoms blooming as a result of iron enrichment appear weakly silicified with C:N ratios slightly lower than Redfield, differential remineralization of nitrogen from the sinking particles resulted in a depletion ratio from the water column much larger than Redfield. Such a shift in DIC:NO_3^- ratio over the entire Southern Ocean during periods of enhanced aerosol iron input would have a significant effect on atmospheric carbon dioxide amounts.

The average decreases in pCO_2, corrected for minimal dilution (~80 μatm), suggest that a

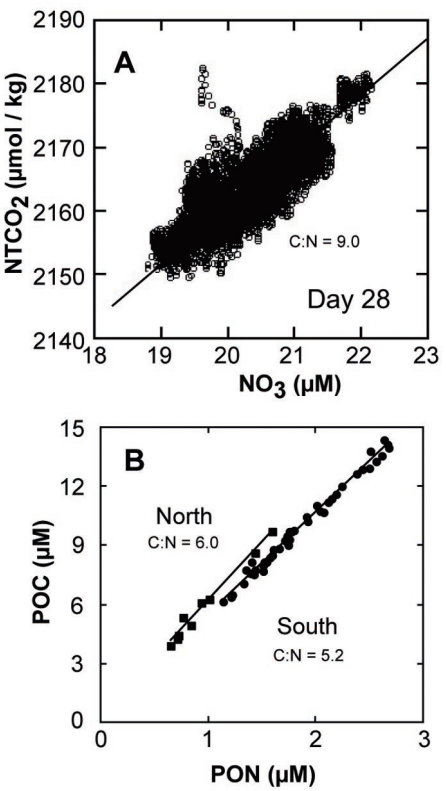

Fig. 6. (**A**) Pumping SeaSoar–derived measurements of TCO_2 and nitrate in the upper 30 m of the north patch. TCO_2 was determined from continuous pCO_2 measurements and observed alkalinity values for the north and south patches, respectively, normalized to a salinity of 35. Sample stream returning through the pumping SeaSoar was analyzed on board *Revelle*. These measurements indicate that non-Redfieldian drawdown ratios of carbon:nitrogen (9.0 ± 0.12) could have supported greater export than expected on the basis of the depletion of nitrate alone. (**B**) Carbon (C) versus nitrogen (N) in suspended particulate material in the mixed layers from both enrichment experiments. North: C = 5.98, N = 0.11, and R^2 = 0.9819. South: C = 5.19, N = 0.24, and R^2 = 0.9899.

glacial-scale enrichment would result in an air-to-sea flux of about 4.6 mol C m^{-2} $year^{-1}$ or about 2 Pg C $year^{-1}$ over an oceanic area of 3.6×10^7 km^2 (50°S to 65°S). Seasonal ice cover may reduce this estimate by a factor of 2. These estimates are several times larger than the present net annual Southern Ocean (south of 50°S) uptake of CO_2 of 0.4 Pg C $year^{-1}$ (*1*) and comparable to the current global ocean net uptake of atmospheric CO_2. Dilution-corrected estimates of POC export (Table 1) extrapolated to an annual basis suggests a similar flux on the order of 8 mol C m^{-2} $year^{-1}$.

These results demonstrate that iron addition to the Southern Ocean increases primary productivity and decreases pCO_2. It remains difficult to extrapolate these findings with confidence to their impact on atmospheric composition because the large-scale impacts of iron enrichment on midwater processes and the length scales of POC remineralization are not yet known. The results strongly suggest, however, that the Southern Ocean was more productive and exported more carbon during periods of higher atmospheric iron input, which occurred during the last glacial maximum.

References and Notes

1. T. Takahashi *et al.*, *Deep-Sea Res. Part II Top. Stud. Oceanogr.* **49**, 1601 (2002).
2. K. L. Daly *et al.*, *J. Geophys. Res.* **106**, 7107 (2001).
3. D. M. Sigman, E. A. Boyle, *Nature* **407**, 859 (2000).
4. K. S. Johnson *et al.*, *Mar. Chem.* **57**, 137 (1997).
5. S. E. Fitzwater *et al.*, *Deep-Sea Res. Part II Top. Stud. Oceanogr.* **47**, 3159 (2000).
6. P. W. Boyd *et al.*, *Nature* **407**, 695 (2000).
7. F. Gervais *et al.*, *Limnol. Oceanogr.* **47**, 1324 (2002).
8. J. H. Martin, *Paleoceanography* **5**, 1 (1990).
9. D. Archer *et al.*, *Rev. Geophys.* **38**, 159 (2000).
10. J. K. Moore *et al.*, *Global Biogeochem. Cycles* **14**, 455 (2000).
11. A. J. Watson *et al.*, *Nature* **407**, 730 (2000).
12. R. F. Anderson, Z. Chase, M. Q. Fleisher, J. Sachs, *Deep-Sea Res. Part II Top. Stud. Oceanogr.* **49**, 1909 (2002).
13. J. R. Petit *et al.*, *Nature* **399**, 429 (1999).
14. R. A. Armstrong *et al.*, *Deep-Sea Res. Part II Top. Stud. Oceanogr.* **49**, 2265 (2002).
15. K. H. Coale *et al.*, *Nature* **383**, 495 (1996).
16. A. Tsuda *et al.*, *Science* **300**, 958 (2003).
17. R. Schlitzer, *EOS* **81**, 45 (2000).
18. M. R. Hiscock *et al.*, *Deep-Sea Res. II* **50**, 533 (2003).
19. T. Trull *et al.*, *Deep-Sea Res. Part II Top. Stud. Oceanogr.* **48**, 2439 (2001).
20. K. H. Coale *et al.*, *Deep-Sea Res. Part II Top. Stud. Oceanogr.* **45**, 919 (1998).
21. Iron enrichments were conducted by R/V Revelle. The northern patch was deployed 10 to 12 January 2002 at 56.23°S and 172°W by injecting 631 kg of iron (as acidic iron sulfate dissolved in seawater) into the ship's wake and spread over an area of 225 km^2. Iron infusions in the north patch of 631 kg and 450 kg were repeated on 16 January and 10 February, respectively. The southern patch was deployed 24 to 26 January at 66.45°S and 171.8°W, with repeated infusions on 29 January, 1 February, and 5 February. Each infusion involved 315 kg spread over a 225 km^2 area. For both patches, initial iron infusions were supplemented with infusions of SF_6 and ^3He as inert chemical tracers. This allowed for rapid detection of the infused area and provided estimates of mixing and gas exchange with the atmosphere. Lagrangian drifter buoys were deployed both inside and outside the enriched areas.
22. K. H. Coale, X. Wang, S. J. Tanner, K. S. Johnson, *Deep-Sea Res. Part II Top. Stud. Oceanogr.* **50**, 635 (2003).
23. K. Johnson *et al.*, *EOS* **83** (suppl.), F799 (2002).
24. E. R. Abraham *et al.*, *Nature* **407**, 727 (2000).
25. P. G. Falkowski, J. A. Raven, *Aquatic Photosynthesis* (Blackwell Scientific, Malden, MA, 1997).
26. M. Behrenfeld *et al.*, *Nature* **371**, 508 (1996).
27. Z. Kolber *et al.*, *Nature* **371**, 145 (1994).
28. P. W. Boyd, E. R. Abraham, *Deep-Sea Res. Part II Top. Stud. Oceanogr.* **48**, 2529 (2001).
29. P. W. Boyd, *Deep-Sea Res. Part II Top. Stud. Oceanogr.* **49**, 1803 (2002).
30. M. R. Landry, R. P. Hassett, *Mar. Biol.* **67**, 283 (1982).
31. M. P. Gall, R. Strzepet, M. Maldonado, P. W. Boyd, *Deep-Sea Res. Part II Top. Stud. Oceanogr.* **48**, 2571 (2001).
32. M. R. Landry *et al.*, *Mar. Ecol. Prog. Ser.* **201**, 57 (2000).
33. B. S. Twining *et al.*, *Anal. Chem.* **75**, 3806 (2003).
34. S. Takeda, *Nature* **393**, 774 (1998).
35. M. A. Brzezinski *et al.*, *Mar. Ecol. Prog. Ser.* **167**, 89 (1998).
36. M. T. Maldonado, N. M. Price, *Mar. Ecol. Prog. Ser.* **141**, 161 (1996).
37. K. R. Timmermans *et al.*, *Mar. Ecol. Prog. Ser.* **166**, 27 (1998).
38. W. P. Cochlan, D. A. Bronk, K. H. Coale, *Deep-Sea Res. Part II Top. Stud. Oceanogr.* **49**, 3365 (2002).
39. D. A. Hutchins, K. W. Bruland, *Nature* **393**, 561 (1998).
40. M. A. Brzezinski, D. R. Phillips, *Limnol. Oceanogr.* **42**, 856 (1997).
41. R. R. Bidigare *et al.*, *EOS* **83** (suppl.), F798 (2002).
42. K. O. Buesseler *et al.*, *Science* **304**, 414 (2004).
43. J. K. B. Bishop *et al.*, *Science* **304**, 417 (2004).
44. C. Sweeney *et al.*, *Deep-Sea Res. Part II Top. Stud. Oceanogr.* **47**, 3395 (2000).
45. B. Hales, T. Takahashi, *J. Atmos. Ocean. Technol.* **19**, 1096 (2002).
46. W. O. Smith *et al.*, *Deep-Sea Res. Part II Top. Stud. Oceanogr.* **47**, 3073 (2000).
47. S. Levitus, *U.S. World Ocean Atlas* (U.S. Department of Commerce, 1998).
48. R. J. Olson *et al.*, *Deep-Sea Res. Part II Top. Stud. Oceanogr.* **47**, 3181 (2000).
49. V. M. Franck *et al.*, *Deep-Sea Res. Part II Top. Stud. Oceanogr.* **47**, 3315 (2000).

50. We wish to thank the entire SOFeX group, crew, and officers of RV *Revelle*, RV *Melville*, and U.S. Coast Guard Research Ice Breaker *Polar Star* and two very thorough reviewers. This research was supported by grants from NSF, Chemical and Biological Oceanography, and U.S. Department of Energy, Office of Science, Biological and Environmental Research.

Supporting Online Material

www.sciencemag.org/cgi/content/full/304/5669/408/DC1
Materials and Methods
Figs. S1 to S5
Tables S1 and S2
References

29 July 2003; accepted 25 March 2004

REPORTS

The Effects of Iron Fertilization on Carbon Sequestration in the Southern Ocean

Ken O. Buesseler,* John E. Andrews, Steven M. Pike, Matthew A. Charette

An unresolved issue in ocean and climate sciences is whether changes to the surface ocean input of the micronutrient iron can alter the flux of carbon to the deep ocean. During the Southern Ocean Iron Experiment, we measured an increase in the flux of particulate carbon from the surface mixed layer, as well as changes in particle cycling below the iron-fertilized patch. The flux of carbon was similar in magnitude to that of natural blooms in the Southern Ocean and thus small relative to global carbon budgets and proposed geoengineering plans to sequester atmospheric carbon dioxide in the deep sea.

As the largest high nutrient–low chlorophyll region, the Southern Ocean was chosen for a purposeful iron fertilization experiment, SOFeX (Southern Ocean Iron Experiment). The experiment was conducted at two sites both north and south of the Antarctic Polar Front, in low- and high-silicate waters, respectively. We focus here on the "southern patch" where the inert tracer SF_6 and four enrichments of iron were added to a 15 km by 15 km patch (66°S, 172°W), which was tracked and monitored by three ships in a Lagrangian fashion for 1 month in January to February 2002. As in previous experiments (*1–3*), the addition of the essential micronutrient iron led to measurable decreases in dissolved inorganic carbon and nutrients within the surface mixed layer (upper 40 to 50 m) associated with enhanced growth of marine phytoplankton, the details of which are described in the accompanying article by Coale *et al.* (*4*).

Department of Marine Chemistry and Geochemistry, Woods Hole Oceanographic Institution, Woods Hole, MA 02543, USA.

*To whom correspondence should be addressed. E-mail: kbuesseler@whoi.edu